The Journal of Immunology

A Key Role for Redox Signaling in Rapid P2X $_7$ Receptor-Induced IL-1β Processing in Human Monocytes

James Hewinson, Samantha F. Moore, Christian Glover, Andrew G. Watts and Amanda B. MacKenzie

J Immunol 2008; 180:8410-8420; ;
doi: 10.4049/jimmunol.180.12.8410
http://www.jimmunol.org/content/180/12/8410

The Journal of Immunology is published twice each month by
The American Association of Immunologists, Inc.,
1451 Rockville Pike, Suite 650, Rockville, MD 20852

Print ISSN: 0022-1767 Online ISSN: 1550-6606.

A Key Role for Redox Signaling in Rapid $P2X_7$ Receptor-Induced IL-1β Processing in Human Monocytes[1]

James Hewinson, Samantha F. Moore, Christian Glover, Andrew G. Watts, and Amanda B. MacKenzie[2]

$P2X_7$ receptors ($P2X_7Rs$) are ATP-gated ion channels that trigger caspase-1 activation in the presence of TLR ligands. Inflammatory caspase-1 is responsible for the proteolytic activation of IL-1β. However, the signaling events that couple $P2X_7Rs$ to caspase-1 activation remain undefined. In this study we demonstrate that ATP-induced cellular oxidation is critical for caspase-1 activation and subsequent IL-1β processing. Purinergic receptor stimulation, including $P2X_7Rs$, of endotoxin-primed human monocytes augments NADPH oxidase activity whereas concurrent purinergic receptor stimulation triggers protein denitroysation, leading to the formation of peroxynitrite. IL-1β cleavage is blocked under conditions where superoxide anion formation is blocked or monocytes are treated with antioxidants or a peroxynitrite scavenger. Nigericin, a K^+/H^+ antiporter, also increases NADPH oxidase activity, leading to IL-1β and caspase-1 processing that is blocked by a peroxynitrite scavenger or inhibition of NADPH oxidase. These data demonstrate that signaling via NADPH oxidase activity is fundamental for the processing of mature IL-1β induced by $P2X_7R$ stimulation. ***The Journal of Immunology,*** **2008, 180: 8410–8420.**

Caspase-1 is a highly regulated cysteine-dependent protease that plays an essential role in host defense and the execution of the innate immune response (1). Indeed, caspase-1-deficient mice exhibit increased susceptibility to bacterial infection and protection against a number of inflammatory diseases (2, 3). The crystal structure of caspase-1 was reported in the mid-1990s; the active site is formed from a dimer of catalytic domains, each containing a p10 and p20 cleavage product of procaspase-1 (4, 5). Mutagenesis studies have revealed that His^{237} and Cys^{285} are critical residues within the active site of the enzyme, where cysteine-reactive compounds can also alter the activity of the wild-type enzyme (4). Caspase-1 is activated within a macromolecular assembly termed the inflammasome, which is constructed from members of the NOD-LRR (nucleotide-binding oligomerization domain leucine-rich repeat) class of proteins (6–8). A series of gene knockout studies have identified a number of different inflammasome assemblies that respond to different pathogenic stimuli. Cytosolic translocation of bacterial flagellin is the only known stimuli of an Ipaf-containing inflammasome (8, 9). By contrast, the inflammasome containing NALP3 (cryopyrin) is assembled in response to a broad range of stimuli (7). For example, macrophages or dendritic cells "primed" by endotoxin stimulation of membrane-associated TLRs leads to the expression of p31 pro-IL-1β and an inflammasome accessory protein, ASC. A second stimulus engages caspase-1 activation, leading to rapid pro-IL-1β processing and secretion of mature 17-kDa IL-1β. Extracellular ATP acting at ionotropic $P2X_7$ receptors ($P2X_7Rs$),[3] pore-forming toxins, or a K^+/H^+ ionophore, nigericin, can act as this second signal (7). Other stimuli of the cryopryin inflammasome include intracellular bacteria, monosodium urate, antiviral compounds, bacterial RNA, or viral dsDNA (10–12).

However, despite the recent advances in the understanding of accessory proteins required for full activation of caspase-1 and the long-standing characterization of the crystal structure, relatively little is known about the signaling pathways that trigger inflammasome activation. In this study we focus on the signaling events coupling ATP-gated $P2X_7Rs$ to rapid caspase-1 activation and subsequent pro-IL-1β processing. The $P2X_7R$ is an atypical member of the P2XR family in which receptor stimulation opens an intrinsic ion channel followed by recruitment of a hemichannel protein, pannexin-1 (13, 14). $P2X_7R$-deficient macrophages fail to process and secrete IL-1β in response to ATP, demonstrating the key role of this purinergic receptor (15, 16). Moreover, transgenic $P2X_7{}^{-/-}$ mice display aberrant bone formation (17) and partial protection against collagen-induced arthritis. As such, $P2X_7Rs$ are emerging as an attractive target for anti-inflammatory drug therapies. It is widely accepted that cytosolic potassium is the key signaling molecule that initiates caspase-1 activation via K^+ efflux from the cell. Evidence for this pathway is largely based on the ability of elevated extracellular K^+ to prevent NALP3 inflammasome activation or enzyme activity assays in low K^+ salines (18, 19). Recent data suggests that a second pathway, involving NADPH oxidase, may contribute to caspase-1 activation. First, an in vivo model of stress led to the

Department of Pharmacy and Pharmacology, University of Bath, Bath, United Kingdom

Received for publication October 9, 2007. Accepted for publication April 10, 2008.

The costs of publication of this article were defrayed in part by the payment of page charges. This article must therefore be hereby marked *advertisement* in accordance with 18 U.S.C. Section 1734 solely to indicate this fact.

[1] This work was supported by grants from British Heart Foundation and Heart Research U.K.

[2] Address correspondence and reprint requests to Dr. Amanda B. MacKenzie, University of Bath, Claverton Down, Bath BA2 7AY, U.K. E-mail address: a.mackenzie@bath.ac.uk

[3] Abbreviations used in this paper: $P2X_7R$, $P2X_7$ receptor; DCF, 2′,7′-dichlorofluorescein; DCFH, 2′,7′-dichlorodihydrofluorescein; DCFH-DA, DCFH diacetate; DPI, diphenyleneiodonium; EtBr, ethidium bromide; FeTPPS, 5,10,15,20-tetrakis(4-sulfonatophenyl)porphyrinato iron (III) chloride; KN-04, *N*-[1-[*N*-methyl-*p*-(5 isoquinolinesulfonyl)benzyl]]-2-(4-phenylpiperazine)ethyl]-5-isoquinoline-sulfonamide; NAC, *N*-acetyl cysteine; NOS, NO synthase; RONS, reactive oxygen and nitrogen species; SOD, superoxide dismutase; z-YVAD-fmk, Tyr-Val-Ala-Asp-fluoromethyl ketone.

generation of mature IL-1β via diphenyleneiodonium (DPI)-sensitive superoxide anion generation (20). Second, caspase-1 activation triggered by endotoxin-sensitized hypoxic-ischemic brain injury was attenuated by the antioxidant *N*-acetylcysteine (NAC) (21). Third, R837 (a synthetic imidazoquinoline compound mimicking ssRNA or ssDNA) or monosodium urate-induced caspase-1 activation was also blocked by the antioxidant NAC (19). Finally, rac1, a component of the NADPH oxidase complex, is implicated in the activation of caspase-1 and generation of mature IL-1β (22).

Several studies in a range of immune cells have reported $P2X_7R$-dependent NADPH oxidase activation resulting in the rapid generation of superoxide anions. In the current study we provide compelling evidence for the role of NADPH oxidase in rapid caspase-1 activation, leading to the processing of pro-IL-1β into mature IL-1β. We also provide evidence that nigericin, a K^+/H^+ ionophore, augments NADPH oxidase activity, leading to caspase-1 activation and IL-1β processing.

Materials and Methods

Reagents and solutions

Unless stated, all reagents were obtained from Sigma Aldrich. 5,10,15,20-Tetrakis(4-sulfonatophenyl)porphyrinato iron (III) chloride (FeTPPS) was obtained from Calbiochem. *N*-[1-[*N*-methyl-*p*-(5 isoquinoline-sulfonyl) benzyl]]-2-(4-phenylpiperazine)ethyl]-5-isoquinoline-sulfonamide (KN-04) and *N*-benzyloxycarbonyl-Tyr-Val-Ala-Asp-fluoromethyl ketone (z-YVAD-fmk) were purchased from D. Western Therapeutics Institute and BioVision, respectively. 2′,7′-dichlorodihydrofluorescein (DCFH) diacetate (DCFH-DA), dihydroethidium, DMEM:Ham's F12 without L-glutamine, FBS, L-glutamine, and penicillin/streptomycin were supplied by Invitrogen. IFN-γ was purchased from Peprotech, the Bio-Rad protein assay from Bio-Rad Laboratories, and Ficoll-Paque Premium from GE Healthcare. The human $P2X_7R$ antagonist AZ11645373 was synthesized as described previously (23, 24). Unless indicated, all experiments were performed in a physiological saline containing 130 mM NaCl, 5 mM KCl, 1.5 mM $CaCl_2$, 1 mM $MgCl_2$, 5 mM $NaHCO_3$, 1.5 mM KH_2PO_4, 25 mM HEPES, and 10 mM D-glucose (pH 7.3; with NaOH).

Cell culture

The human monocytic cell line THP-1 (American Type Culture Collection) was maintained in suspension culture at a density of 5×10^4 to 1×10^6 cells ml^{-1} in DMEM:F-12 containing 10% heat inactivated FBS, 2 mM L-glutamine, 100 U ml^{-1} penicillin, and 100 μg ml^{-1} streptomycin (complete medium). THP-1 cells were incubated in a humidified atmosphere of 95% air and 5% CO_2. THP-1 cells were differentiated into macrophage-like cells by overnight incubation in complete culture medium containing 10 ng ml^{-1} IFN-γ and 25 ng ml^{-1} LPS. For use in fluorescence-based assays THP-1 cells were plated into black 96-well plates (1.5×10^5 cells/well). To obtain samples for Western Blot analysis, cells were plated in 6-well plates (3×10^6 cells/well). Primary human monocytes were isolated from blood obtained from healthy volunteers, the buffy coat was collected using a Ficoll gradient, and monocytes were enriched by adherence to tissue culture plastic. Monocytes were cultured overnight in complete medium (as described for THP-1 cells) and activated with 1 μg ml^{-1} LPS for 6 h before stimulation with extracellular ATP.

Fluorescence assays

Reactive oxygen and nitrogen species (RONS) generation was detected in cells loaded with the RONS-sensitive compound DCFH-DA. Differentiated THP-1 cells or primary human monocytes were incubated with 10 μM DCFH-DA in DMEM:F12 (not containing supplements) for 40 min at ambient room temperature and under limited light conditions. DCFH-loaded cells were stimulated in physiological saline and 2′,7′-dichlorofluorescein (DCF) fluorescence was collected at 37°C using a FLUOstar OPTIMA multiwell plate reader (BMG Labtech); DCF excitation and emission wavelengths were 485 nm and 520 nm, respectively. DCFH-DA is a fluorescein-based dye sensitive to changes in intracellular pH. Addition of nigericin, a K^+/H^+ ionophore, will alter intracellular pH where DCFH would not be suitable to measure any changes in cellular oxidation. Instead, we have measured superoxide anion generation by using dihydroethidium, where THP-1 cells were stimulated in the presence of 10 μM dihydroethidium in a physiological saline in the absence or presence of inhibitors or enzymes. Dihydroethidium excitation and emission wavelengths were 544 and 590 nm, respectively.

Stimulation of the $P2X_7R$ is known to induce the formation of a pore in the plasma membrane permeable to high molecular mass molecules $\leq$ 1000 Da. To assess pore-formation as an indication of functional $P2X_7R$ expression, the uptake of ethidium bromide (EtBr; molecular mass of 394 Da) was measured. EtBr fluorescence was recorded using a FLUOstar OPTIMA multiwell plate reader at 37 °C with excitation and emission wavelengths of 544 and 590 nm, respectively. THP-1 or primary human monocytes were plated into black 96-well plates and differentiated as previously described. The culture medium was replaced with PBS and 25 μM EtBr (prepared in PBS) was added immediately before recordings.

Western blot analysis

Differentiated THP-1 cells or LPS-primed (1 μg ml^{-1} for 6 h) primary human monocytes were washed once in physiological saline and stimulated with 5 mM ATP or 10 μM nigericin in the presence of inhibitors at 37°C. Physiological saline above the cells was collected for analysis of secreted proteins and, following a wash step in ice-cold physiological saline, cells were lysed in 250 μl of protease inhibitor mixture plus 1% Triton X-100. Lysates and secreted protein fractions were cleared by centrifugation at $1500 \times g$ for 10 min. Secreted protein fractions were subsequently concentrated ($\times$10) using 3-kDa cut-off filters according to manufacturers instructions (Pall Process Filtration). Proteins were resolved by electrophoresis on 12% SDS-polyacrylamide gels and transferred onto nitrocellulose membrane. Primary Abs were developed with HRP-conjugated secondary Abs and immune complexes were detected using ECL. Abs raised against IL-1β and caspase-1 were obtained from Endogen and Cell Signaling Technology, respectively.

NADPH oxidase subunit membrane translocation

THP-1 cells were differentiated overnight (3×10^6 cells per well of a 24-well plate) and complete medium was replaced with physiological saline before treatments. Following ATP stimulation, plates were incubated on ice and cells were dissociated into saline using a cell scraper. Cells were disrupted using a Constant cell disruption system (Constant Systems) set at 30,000 pounds per square inch. Cells lysates were cleared by centrifugation at $1,500 \times g$ for 15 min and the resulting supernatant was subjected to further centrifugation at $100,000 \times g$ for 30 min using a Beckman L8–70M ultracentrifuge (Rotor Type 70.1 T1; Beckman Coulter). The pellet (membrane fraction) was dissolved in sample buffer and the supernatant (cell lysate) was mixed with an equal volume of 2$\times$ sample buffer. $p67^{phox}$ protein content was analyzed by Western blotting using an Ab obtained from BD Biosciences.

$p67^{phox}$ immunoprecipitation

Media was removed from differentiated THP-1 cells (in 6-well plates; 3×10^6 cells per well) and the cells were washed once in physiological saline at 37°C. THP-1 cells were stimulated with 5 mM ATP at 37°C and lysed by the addition of ice-cold protease inhibitor mixture plus 1% Triton X-100, 20 μM sodium orthovanadate, 200 μM sodium fluoride, and 4 μM phenylmethanesulfonyl fluoride. Cell lysates were cleared by centrifugation at $1500 \times g$ for 10 min, incubated with 1 μg of anti-$p67^{phox}$ (BD Biosciences) for 1–2 h at 4 °C, and subsequently with 20 μl of protein A/G PLUS-Agarose (Santa Cruz Biotechnology) for 1–2 h at 4°C with continuous agitation. Agarose beads were washed three times in ice-cold PBS ($1000 \times g$ for 5-min centrifugation steps at 4°C). Following the final wash step, the agarose-bead pellet was resuspended in sample buffer and boiled for 5 min before resolution using SDS-PAGE. $p67^{phox}$-immunoprecipitated samples were immunoblotted for $p47^{phox}$ (Upstate Biotechnology).

S-*Nitrosylation quantification with Saville-Griess assay*

LPS- and IFN-γ-differentiated THP-1 cells were incubated at 37°C with ATP in physiological saline. Extracellular saline was collected for analysis and cells were lysed in ice-cold lysis buffer containing 1% Nonidet P-40 and a protease inhibitor mixture. Samples were split into two and either left untreated or incubated with 1 mM mercury chloride for 10 min at room temperature to displace NO from SNO groups. Griess reagent was incubated with the samples (1:1) and nitrite concentrations were determined from sodium nitrite standard curves quantified on a plate reader at 544 nm. Sample protein concentrations were measured using the Bio-Rad protein assay following the manufacturer's instructions.

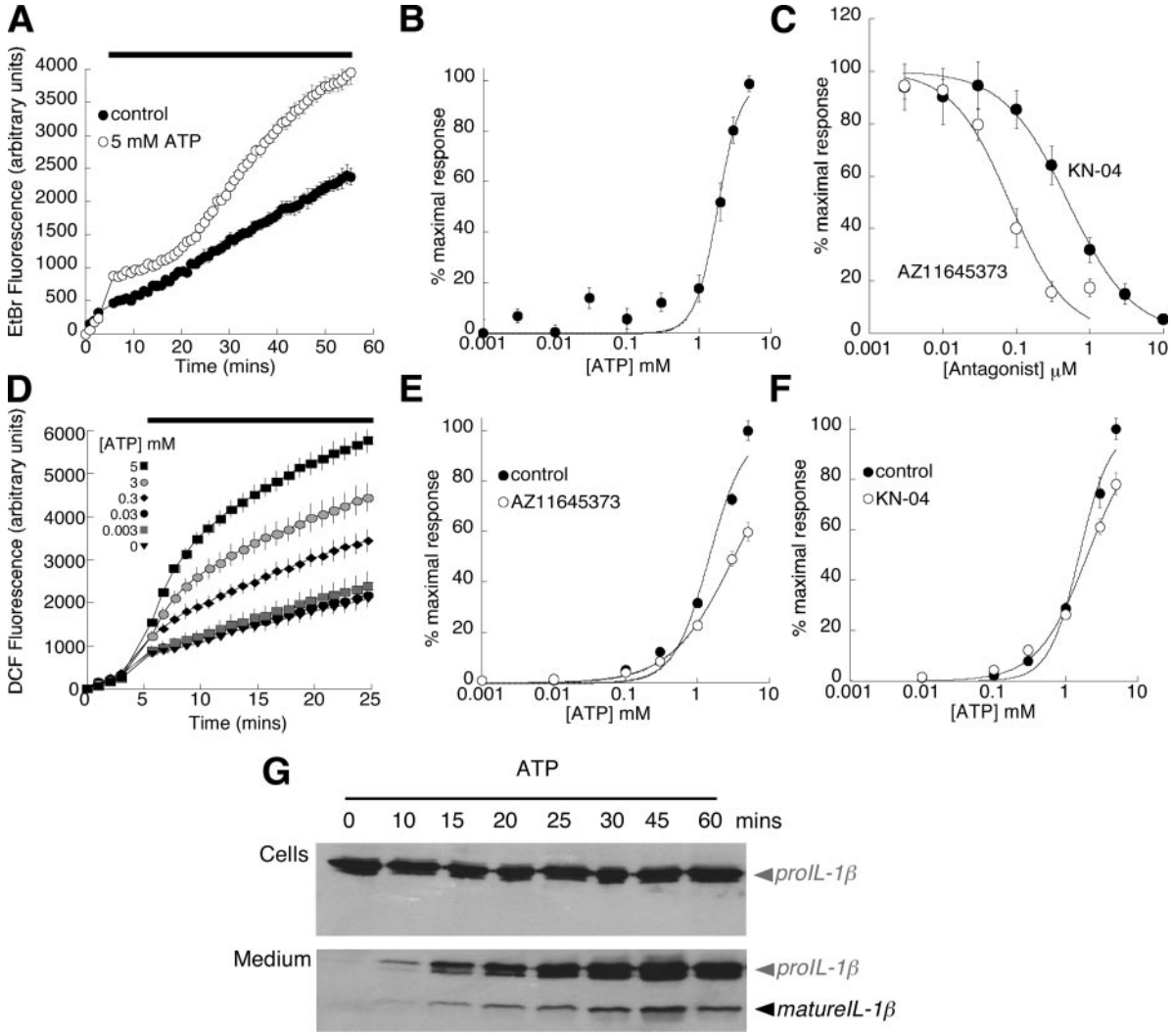

FIGURE 1. ATP stimulation couples to rapid RONS generation. *A*, ATP-mediated EtBr influx in THP-1 cells measured at excitation and emission wavelengths of 544 nm and 590 nm, respectively. Filled circles represent the addition of buffer in control experiments and the open circles represent the addition of 5 mM ATP. Agonist addition is indicated by the horizontal bar. *B*, ATP dose response for EtBr influx into THP-1 cells. Rates were calculated from initial linear increases in fluorescence and normalized to the maximal response. *C*, Preincubation (5 min) with AZ11645373 (open circles) or KN-04 (filled circles) causes a dose-dependent inhibition of 3 mM ATP-induced EtBr influx. *D*, ATP-induced RONS generation in DCFH-loaded THP-1 was measured at excitation and emission wavelengths of 485 nm and 520 nm, respectively. ATP concentrations are indicated within the graph. *E* and *F*, RONS generation rates were calculated from initial linear increases in fluorescence and normalized to the maximal response. Both processes are ATP dose dependent. *E*, Preincubation of THP-1 cells with 10 μM AZ11645373 (5 min) caused an inhibition of ATP-induced RONS (open circles) compared with control responses (filled circles). *F*, Preincubation of THP-1 cells with 1 μM KN-04 (5 min) caused an inhibition of ATP-induced RONS (open circles) compared with control responses (filled circles). *G*, THP-1 cells were incubated with ATP (5 mM) and lysates and concentrated secreted proteins were probed for IL-1β using immunoblotting. Incubation of THP-1 with 5 mM ATP induces time-dependent processing and release of IL-1β with the release of mature IL-1β (17 kDa) evident at 10 min and a peak at 45 min of ATP stimulation ($n = 3$ separate experiments). *Upper panel*, Cell lysate; *lower panel*, concentrated secreted protein. All values are mean ± SEM.

Data analysis and statistics

All data points shown represent the mean ± SEM with a minimum of three independent experiments. Densitometry measurements were performed with NIH Image 1.63 software. Data were analyzed by one-way ANOVA with Dunnett's post-test or unpaired two-tailed *t* test using GraphPad Prism Version 4.0c (GraphPad Software). Agonist dose-response curves were fit using $R/R_{max} = 100([A]^{nH}/([A]^{nH} + EC_{50}{}^{nH})$, where [*A*] represents agonist concentration, *R* is the fluorescence response induced by [*A*] expressed as a function of the peak maximal agonist response (R_{max}), n_H is the Hill coefficient, EC_{50} the half maximal response and pD_2 the negative logarithm to base 10 of the EC_{50} value. Inhibition curves were fit by $R/R_{max} = 100([B]^{nH}/([B]^{nH} + IC_{50}{}^{nH})$ where [*B*] corresponds to the concentration of the antagonist and IC_{50} is the concentration of the antagonist required for a reduction of agonist response by 50%.

Results

Extracellular ATP triggers rapid cellular oxidation and IL-1β processing in human THP-1 cells

ATP-gated $P2X_7Rs$ are coupled to the opening of a large pore in the plasma membrane, permeable to large molecular mass dyes, recently identified as the hemichannel pannexin-1 (13). The influx of EtBr (394 Da) was used to detect pore formation, upon the addition of extracellular ATP, as an indicator of functional $P2X_7Rs$. The addition of 5 mM ATP induced the influx of EtBr with a delay of 15 min that increased over the 30-min recording period (Fig. 1*A*). The ATP concentration response curve gave an EC_{50} value of 1.97 mM ($pD_2 = 2.74 \pm 0.07$; $n = 6$) (Fig. 1*B*).

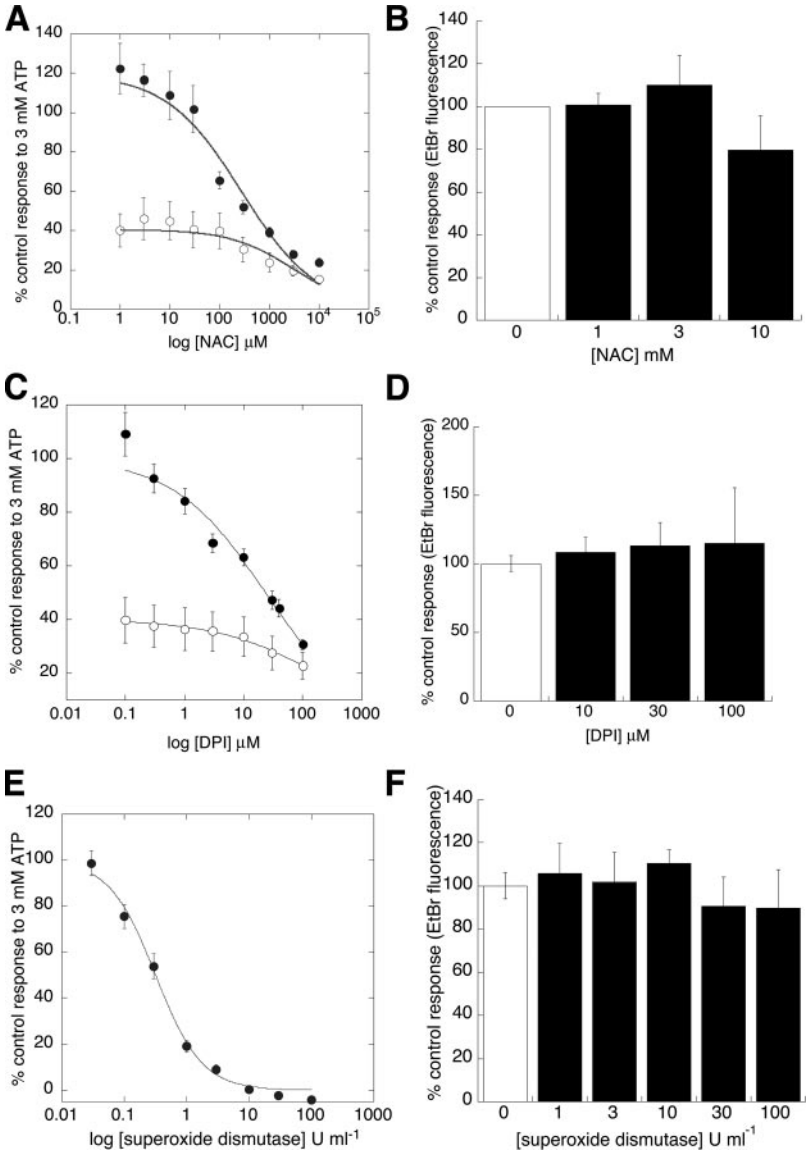

FIGURE 2. $P2X_7R$ stimulation modulates NADPH oxidase activity and peroxynitrite generation. Preincubation of THP-1 cells with NAC for 2 h (*A*), DPI for 1.5 h (*C*), or SOD for 5 min (*E*) inhibits 3 mM ATP-induced RONS detection (filled circles) to buffer control levels (open circles). At the concentrations tested, these compounds do not effect pore formation (*B*, *D*, and *F*). Data were analyzed as described in the legend to Fig. 1.

Selective human $P2X_7R$ antagonists blocked the ATP-evoked pore formation, where AZ11645373 blocked with an IC_{50} value of 95 nM ($n = 4$) or KN-04 with an IC_{50} value of 534 nM ($n = 3$) (Fig. 1*C*). Application of extracellular ATP to LPS-primed THP-1 macrophages also caused a burst in oxidation followed by a sustained increase over 20 min (Fig. 1*D*). The concentration response of the initial burst (approximately within the first 5 min of recording following ATP application) gave an EC_{50} value of 1.59–1.62 mM ($pD_2 = 2.80 \pm 0.02$ to 2.79 ± 0.02; $n = 4$) (Fig. 1, *E* and *F*), comparable to reported values for human $P2X_7Rs$ (25). By contrast, ATP-induced oxidation was only partially blocked by 10 μM AZ11645373 (40% inhibition of 5 mM ATP response) or 1 μM KN-04 (22% inhibition of 5 mM ATP response) (Fig. 1, *E* and *F*). Previously, the $P2X_7R$ has been reported to couple to the rapid processing and secretion of mature IL-1β within 30 min of receptor activation (13, 26, 27). We asked whether there was a temporal correlation between cellular oxidation and IL-1β processing. Application of extracellular ATP caused generation of mature IL-1β within 10 min, detected in the external medium as a 17-kD protein (Fig. 1*G*). The ATP-dependent burst in oxidation occurs in the first 5 min of agonist application, before the detection of mature IL-1β. We have investigated whether cellular oxidation, albeit partially $P2X_7R$ dependent, contributes to ATP-mediated rapid processing of pro-IL-1β.

ATP-gated $P2X_7Rs$ activate NADPH oxidase

The fluorescent indicator DCF detects a range of cellular oxidants including peroxynitrite, hydroxyl radicals, and hydrogen peroxide (28, 29). First, we have characterized the reactive oxygen species detected by DCF in response to ATP stimulation. The antioxidant NAC is converted into glutathione that reacts with cellular oxidants including hydrogen peroxide and peroxynitrite (30, 31). LPS-primed macrophages were loaded with NAC for 2 h before recordings; NAC loading resulted in a concentration-dependent block of ATP-triggered increases in DCF fluorescence (IC_{50}, 86 μM; pD_2, 4.07 ± 0.03; $n = 3$), indicating that the signal is mediated by cellular oxidation (Fig. 2*A*).

Several mechanisms may account for the increase in cellular oxidation upon exposure to high concentrations of extracellular ATP. $P2X_7Rs$ have previously been reported to couple to plasmalemmal NADPH oxidase to trigger the rapid generation of superoxide anions (32). The NADPH oxidase inhibitor DPI inhibited ATP mediated cellular oxidation with an IC_{50} value of 11.7 μM (pD_2, 5.05 ± 0.2; $n = 5$) (Fig. 2*C*). DPI is not completely selective

for plasma membrane NADPH oxidase and also blocks mitochondrial NADH dehydrogenases, leading to a potential inhibition of mitochondrial respiration (33). Treatment of cells with inhibitors of mitochondrial respiration, rotenone or myxothiazol (≤ 1 μM), did not inhibit ATP-mediated cellular oxidation (data not shown). Alternatively, DPI may also inhibit xanthine oxidase and also lead to a decreased generation of cytosolic superoxide anions (34). However ATP-mediated cellular oxidation was not blocked by preincubation with the xanthine oxidase inhibitor allopurinol (≤ 30 μM) (data not shown). Translocation to the plasma membrane and the activation of NADPH oxidase would result in the liberation of superoxide anions into the external environment. Superoxide dismutase (SOD) is an enzyme that rapidly dismutates superoxide anions into hydrogen peroxide. The addition of extracellular SOD to scavenge superoxide anions led to an inhibition of ATP-mediated cellular oxidation (IC_{50}, 0.33 U ml^{-1}; $n = 4$) (Fig. 2*E*), indicating an extracellular source of superoxide anions. In parallel experiments, all the above enzymes, amino acids, or inhibitors were tested on P2X$_7$R-induced EtBr uptake. None of the above conditions (NAC, DPI, or SOD) were found to block P2X$_7$R-induced EtBr influx (Fig. 2, *B*, *D*, and *F*). These data demonstrate that RONS formation does not modulate P2X$_7$R-mediated pore formation and EtBr influx and, therefore, the receptor itself.

Activation of NADPH oxidase involves the translocation of cytosolic components (p47^{phox}, p40^{phox}, p67^{phox}, and p21^{rac}) onto membrane-bound proteins (gp91^{phox} and gp22^{phox}), forming a macromolecular complex. The interaction between p67^{phox} and p47^{phox}, the adaptor component, leads to the recruitment of p67^{phox} to the membrane-spanning components via the interaction of p47^{phox} with membrane lipids (35). Coimmunoprecipition of p67^{phox} followed by Western blot analysis for interacting proteins demonstrates an interaction with p47^{phox} upon ATP stimulation of primed THP-1 cell lysates (Fig. 3*A*). The priming of THP-1 cells with LPS alone leads to translocation of p67^{phox} (Fig. 3*B*). Membrane translocation of p67^{phox} was enhanced upon stimulation with 5 mM ATP (Fig. 3*C*). The ATP-dependent translocation of p67^{phox} was attenuated by preincubation with 10 μM AZ11645373, a human P2X$_7$R antagonist (Fig. 3*D*).

Evidence for extracellular ATP-dependent release of NO from S-nitrosothiol

Superoxide anions can rapidly combine with NO to form peroxynitrite that is readily detectable by the fluorescent dye DCF. The inhibitory action of SOD would suggest the formation of the oxidant peroxynitrite. In support of this conclusion, the addition of catalase (an enzyme that degrades hydrogen peroxide) did not block ATP-mediated increases in cellular oxidation (data not shown). We tested the action of a peroxynitrite scavenger, FeTPPS, on caspase-1 activation. However, we found that this reagent interfered with the fluorescent output of DCF (J. Hewinson and A. B. MacKenzie, unpublished observations). We investigated the potential source of NO that would combine with superoxide anions to form peroxynitrite. First we evaluated the contribution of NO synthesis from the enzyme NO synthase (NOS). Incubation of cells with up to 100 μM N^G-nitro-L-arginine methyl ester hydrochloride, a broad-spectrum NOS inhibitor, or up to 3 μM 1400W, an iNOS inhibitor, did not attenuate the ATP-dependent increase in DCF fluorescence ($n = 3$) (Fig. 4*A*). The lack of action of NOS inhibitors would indicate an alternative source of NO during ATP stimulation. A second mechanism for NO release has been proposed in a range of cells, including pancreatic acinar cells and dorsal root ganglia, where NO is liberated from *S*-nitrosylated proteins (36). NO, in the presence of an electron acceptor, can react with cysteine thiol groups to form an SNO bond. We investigated

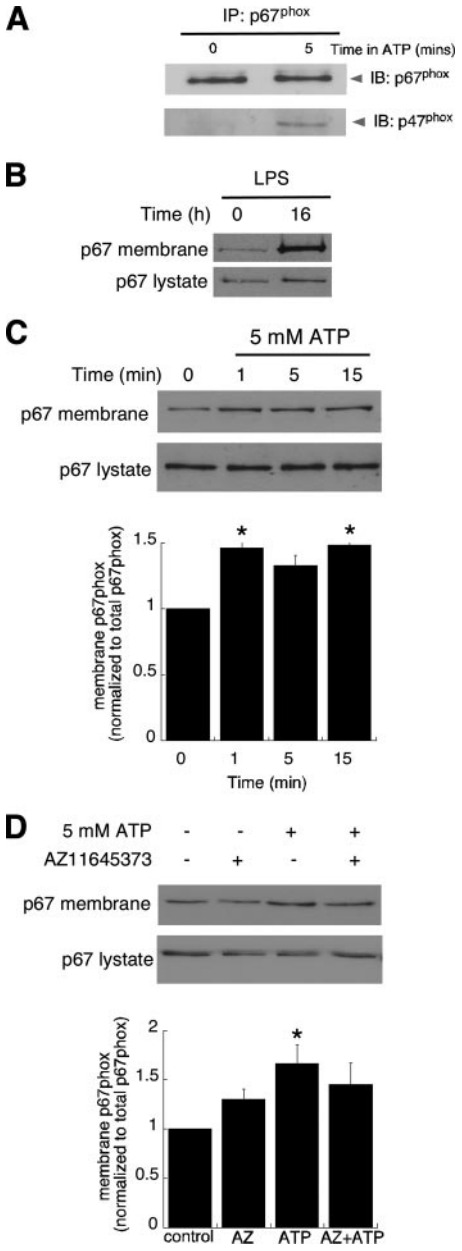

FIGURE 3. ATP stimulation induces assembly of NADPH oxidase. *A*, p67^{phox} was immunoprecipitated (IP) from lysates of 5 mM ATP-stimulated THP-1 cells and immunoblotted (IB) for the p47^{phox} subunit. *B*, Membrane preparations from control and LPS-stimulated THP-1 cells were prepared and immunoblotted for p67^{phox}. *C*, Membrane preparations from ATP-stimulated LPS-primed THP-1 cells were prepared and immunoblotted for p67^{phox}. Density measurements were taken, the ratio of membrane-associated vs total p67^{phox} density was calculated, and individual experiments were standardized to the control ratio. *D*, THP-1 cells were pretreated with 10 μM AZ11645373 (AZ) for 5 min and stimulated with 5 mM ATP for 5 min. Membrane preparations were analyzed as described in *B*. All values are mean ± SEM; $n = 3$ separate experiments.

intracellular SNO protein content using the Saville reaction where the addition of mercury to cell lysates will cleave the SNO bond and liberate nitrite ions (37). The addition of extracellular ATP led to a time-dependent decrease in SNO groups on cytosolic proteins (Fig. 4*B*). Extracellular ATP ranging from 1 μM to 5 mM could trigger protein denitrosylation (Fig. 4*C*). We propose that ATP stimulation triggers the liberation of NO from SNO proteins and is the source of NO to form peroxynitrite.

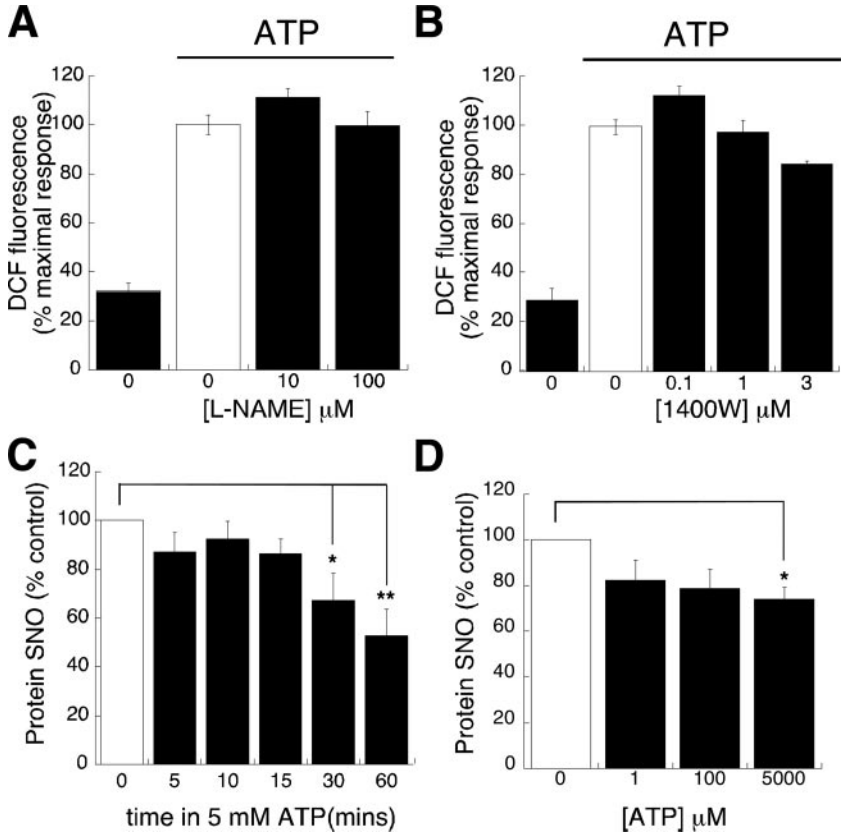

FIGURE 4. ATP-induced peroxynitrite formation does not require NOS activity. Differentiated THP-1 cells were incubated with N^G-nitro-L-arginine methyl ester hydrochloride (L-NAME) (*A*) or 1400W (*B*) for 60 min. ATP-induced RONS generation rates were recorded and normalized to ATP-evoked RONS generation in the absence of inhibitor. *C* and *D*, Differentiated THP-1 cells were incubated with ATP as indicated. Levels of mercury-displaceable protein *S*-nitrosylation were measured in cell lysates using Saville-Griess reagent and standardized to buffer control. Data were analyzed using one-way ANOVA with Dunnett's post-test. All values are mean ± SEM; $n = 3$–7 separate experiments. *, $p < 0.05$; **, $p < 0.01$.

Cellular oxidation mediates rapid P2X$_7$R-dependent IL-1β processing

Peroxynitrite can alter protein function by directly reacting with a number of amino acids in the peptide sequences, including a cysteine oxidation or tyrosine nitration (38). Peroxynitrite-mediated protein modifications are reported to mediate a range of signaling events, including changes in enzyme activity or protein-protein interactions. Activation of P2X$_7$Rs triggers a rapid burst in peroxynitrite formation that precedes the processing of pro-IL-1β as detected by Western blot analysis (Fig. 1*G*). We asked whether peroxynitrite formation plays an important role in caspase-1 activation leading to the generation and secretion of mature IL-1β.

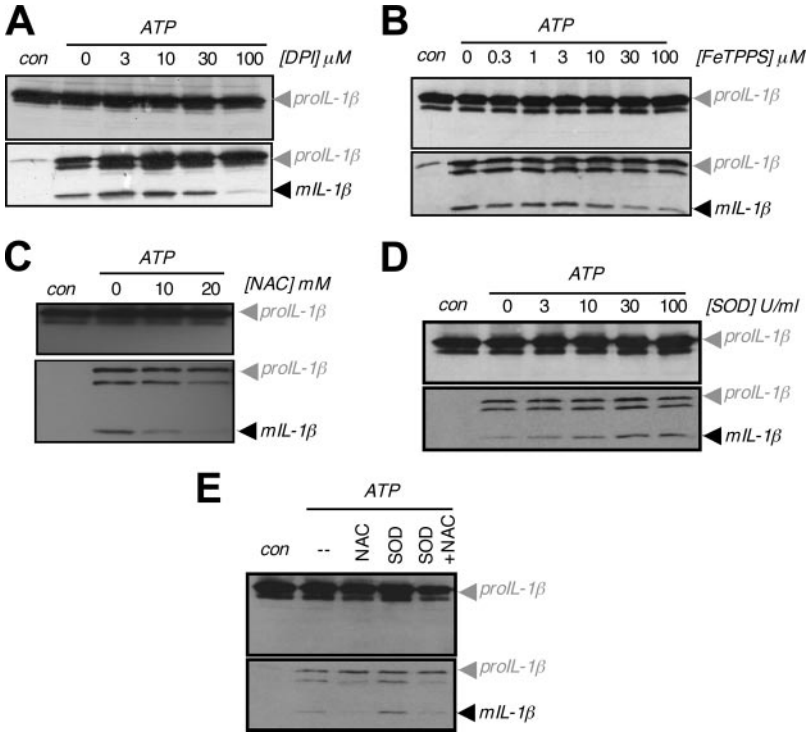

FIGURE 5. P2X$_7$R-dependent IL-1β processing requires NADPH oxidase activity and a pro-oxidant signal. THP-1 cells were preincubated with DPI for 90 min (*A*), FeTPPS for 30 min (*B*), NAC for 120 min (*C*), SOD for 5 min (*D*), or a combination of 20 mM NAC for 120 min and 100 U ml^{-1} SOD for 5 min (*E*), and 5 mM ATP-induced IL-1β processing and secretion were analyzed by immunoblotting. *Upper panel*, cell lysate; *lower panel*, concentrated secreted protein. $n = 3$ separate experiments. con, Control; mIL-1β, mature IL-1β.

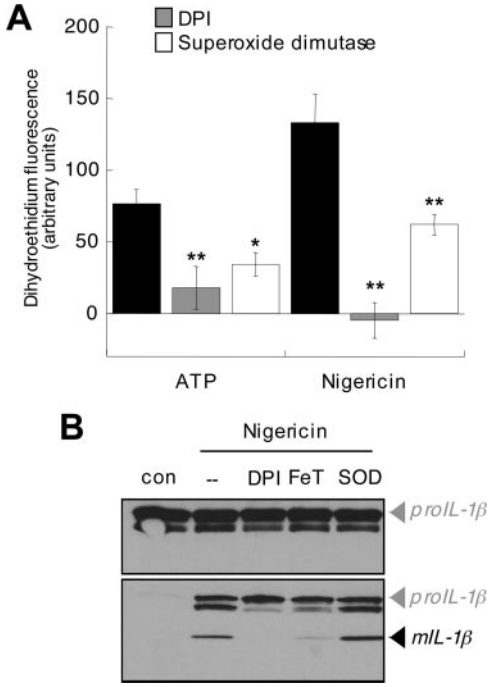

FIGURE 6. Nigericin induces oxidant generation and peroxynitrite-dependent IL-1β processing. *A*, THP-1 cells were preincubated with 100 μM DPI for 90 min or 100 U ml^{-1} SOD for 5 min and 3 mM ATP- or 10 μM nigericin-induced superoxide generation was measured in dihydroethidium-loaded cells at excitation and emission wavelengths of 544 nm and 590 nm, respectively. Paired buffer control values were subtracted and end point fluorescence values (at 15 min of stimulation) are represented. Data were analyzed using one-way ANOVA with Dunnett's post-test. *B*, Differentiated THP-1 cells preincubated with 100 μM DPI for 90 min, 100 μM FeTPPS (FeT) for 30 min, or 100 U ml^{-1} SOD for 5 min were stimulated with 10 μM nigericin for 30 min. IL-1β processing in lysates and concentrated supernatants was analyzed by immunoblotting. *Upper panel*, cell lysate; *lower panel*, medium. All values are mean ± SEM; $n = 3$ separate experiments. *, $p < 0.05$; **, $p < 0.01$. con, Control; mIL-1β, mature IL-1β.

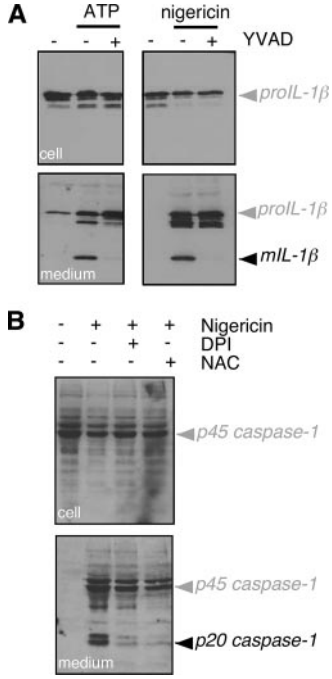

FIGURE 7. Caspase-1 processing is redox dependent. *A*, THP-1 cells were preincubated with 10 μM z-YVAD-fmk for 30 min and 5 mM ATP- (45 min) or 10 μM nigericin-induced (30 min) IL-1β processing and secretion were assessed by immunoblotting. *B*, THP-1 cells were preincubated with 20 mM NAC for 120 min or 100 μM DPI for 90 min and 10 μM nigericin-induced (30 min) caspase-1 processing and secretion were assessed by immunoblotting.

As previously reported, P2X$_7$R induced the secretion of both pro and mature IL-1β into the external medium (13, 26). At the 45-min time point analyzed in these experiments, as determined by densitometry analysis of semiquantitative blots ~20–30% of secreted IL-1β was in the processed 17-kDa form. Pretreatment of LPS-primed THP-1 cells with DPI (100 μM) to inhibit NADPH oxidase blocked the generation of mature IL-1β ($n = 3$; Fig. 5*A*). It is of note that DPI does not block P2X$_7$R-dependent secretion of pro-IL-1β; as such, the inhibitory action was selective for processing and not secretion. From previous experiments, we propose that P2X$_7$R stimulation leads to the formation of peroxynitrite. The treatment of cells with the peroxynitrite scavenger FeTPPS lead to a dose-dependent inhibition of pro-IL-1β processing without blocking secretion (Fig. 5*B*). Loading of macrophages with the antioxidant NAC also inhibited ATP-mediated IL-1β processing without any block of pro-IL-1β secretion into the medium (Fig. 5*C*). Co-addition of extracellular SOD with ATP potentiated IL-1β processing (Fig. 5*D*). This result is in contrast to the recordings of peroxynitrite where the addition of SOD blocked ATP-evoked increases in DCF fluorescence. Under these conditions, SOD would be predicted to dismutate superoxide anions into hydrogen peroxide, weakly detected by DCF. We hypothesize that an oxidative pathway, either due to peroxynitrite or hydrogen peroxide generation, is responsible for ATP-mediated IL-1β processing. In agreement with this theory, preloading of cells with NAC blocked ATP-induced IL-1β processing in the presence of extracellular SOD (Fig. 5*E*).

Cellular oxidation mediates rapid nigericin triggered IL-1β processing

We investigated whether the regulation of caspase-1 by cellular oxidation is restricted to P2X$_7$R-stimulated pathways. A nonphysiological stimulus of caspase-1, the K^+/H^+ antiporter nigericin, triggers rapid processing and secretion of pro-IL-1β. The addition of 10 μM nigericin to differentiated THP-1 cells triggered the generation of superoxide anions detected using dihydroethidium. Nigericin-induced superoxide anion formation was blocked by 100 μM DPI and partially reduced by the addition of external SOD (Fig. 6*A*). Western blot analysis of IL-1β processing confirmed that nigericin stimulation of LPS-primed macrophages triggers IL-1β processing and secretion within 30 min of stimulation. Treatment of primed monocytes with DPI or FeTPPS abolished nigericin-induced IL-1β processing (Fig. 6*B*). The addition of extracellular SOD augmented nigericin-induced IL-1β processing. We conclude that the K^+/H^+ antiporter nigericin augments NADPH oxidase activity to trigger rapid caspase-1 activation and subsequent pro-IL-1β processing.

Cellular oxidation required for caspase-1 processing

For both ATP- and nigericin-stimulated IL-1β processing in THP-1 cells, preincubation with a caspase-1 peptide inhibitor (z-YVAD-fmk) prevented the production of mature IL-1β but did not effect the secretion of pro-IL-1β into the external medium (Fig. 7*A*). Comparable results are observed in the presence of antioxidants (NAC or FeTPPS) or an NADPH oxidase inhibitor (DPI) where the generation of mature IL-1β is blocked but secretion of

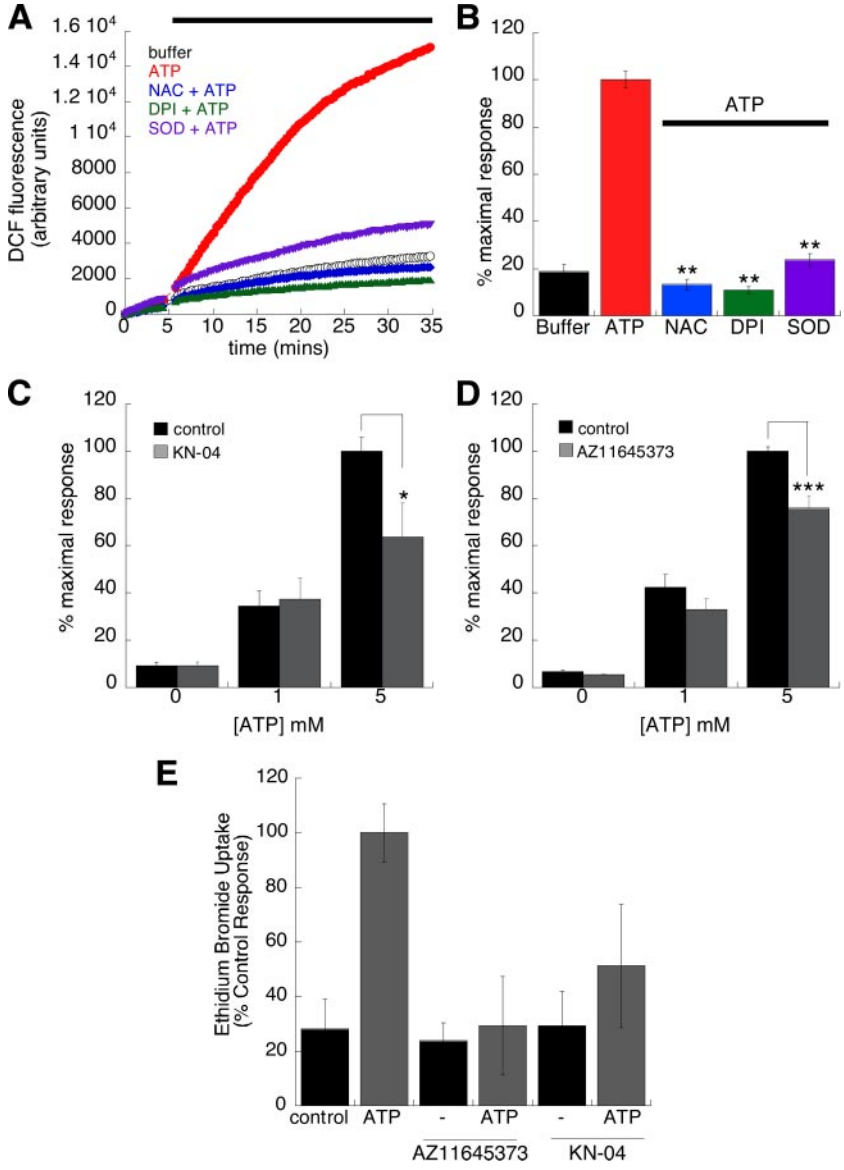

FIGURE 8. ATP stimulation couples to rapid oxidation in human blood-derived monocytes. *A*, Three mM ATP-induced RONS generation was measured in LPS-primed, human blood-derived monocytes preincubated with 20 mM NAC, 100 μM DPI for 90 min, or 100 U ml^{-1} SOD for 5 min. *B*, RONS generation rates were calculated from the initial linear increase in DCF fluorescence and normalized to the ATP control response. Data were plotted for control (Buffer), ATP, and ATP in the presence of DPI, NAC, or SOD as indicated. *C* and *D*, RONS generation rates were calculated in the presence of 1 μM KN-04 (*C*) or 10 μM AZ11645373 (*D*) and normalized to the 5 mM ATP control response. *E*, LPS-primed human blood-derived monocytes were incubated with 1 μM KN-04 or 1 μM AZ11645373 for 5 min. ATP-induced EtBr influx was measured at excitation and emission wavelengths of 544 and 590 nm, respectively. Rates of influx were calculated from linear increases in fluorescence following the addition of ATP and normalized to the ATP control response. Data were analyzed using one-way ANOVA with Dunnett's post-test. All values are mean ± SEM; $n = 3$–5 separate experiments. *, $p < 0.05$; **, $p < 0.01$; ***, $p < 0.001$.

pro-IL-1β is retained (Figs. 5 and 6). We next investigated ATP- and nigericin-stimulated caspase-1 processing in the presence of DPI and NAC. For nigericin, robust rapid caspase-1 processing was detected at 30 min where the generation of the active p20 subunit was attenuated by pretreatment with DPI or NAC (Fig. 7*B*). By contrast, we failed to detect active caspase-1 subunits upon stimulation with extracellular ATP. We hypothesize that either of the following is the reason for this failure: 1) the level of active caspase-1 is below the level of detection by Western blot; or 2) caspase-1 subunits are rapidly degraded by a second protease. In murine J774 macrophages, ATP stimulation triggers the transient appearance of a p10 caspase-1 subunit where the detectable p10 subunit decreases to basal levels following prolonged (45–60 min) receptor stimulation (S. F. Moore and A. B. MacKenzie, unpublished observations). These data may support the hypothesis that active caspase-1 subunits are rapidly degraded following human $P2X_7R$ stimulation. In summary, we have demonstrated that caspase-1 is required for IL-1β processing following nigericin or ATP stimulation, but active caspase-1 subunits are only detectable following nigericin stimulation. Further, cellular oxidation is required for the production of active p20 caspase-1 subunits.

Primary human monocytes

To exclude the possibility that this pathway is unique to THP-1 cells, we repeated these experiments in isolated human monocytes primed with LPS. As illustrated in Fig. 8, the addition of 3 mM ATP triggered a robust increase in DCF fluorescence that was more sustained over the 30-min recording period as opposed to the burst response observed in primed THP-1 cells. ATP-induced RONS generation was attenuated by treatment with DPI, NAC, or the co-addition of extracellular SOD (Fig. 8, *A* and *B*). In agreement with results from THP-1 cells, 10 μM AZ11645373 or 1 μM KN-04 partially blocked ATP-mediated RONS formation by 25 and 36%, respectively (Fig. 8, *C* and *D*). Although 1 μM AZ11645373 or 1 μM KN-04 strongly inhibited EtBr uptake (Fig. 8*E*), LPS-primed monocytes from all donors ($n = 5$) responded to ATP stimulation, leading to the processing and secretion of mature IL-1β. Incubation of monocytes with DPI attenuated pro-IL-1β processing in four donors ($n = 5$), whereas the addition of SOD augmented pro-IL-1β processing in all donors (Fig. 9, *A* and *B*). Of note, FeTPPS attenuated ATP-mediated IL-1β processing in only two of the donors ($n = 5$). The variability in FeTPPS may result

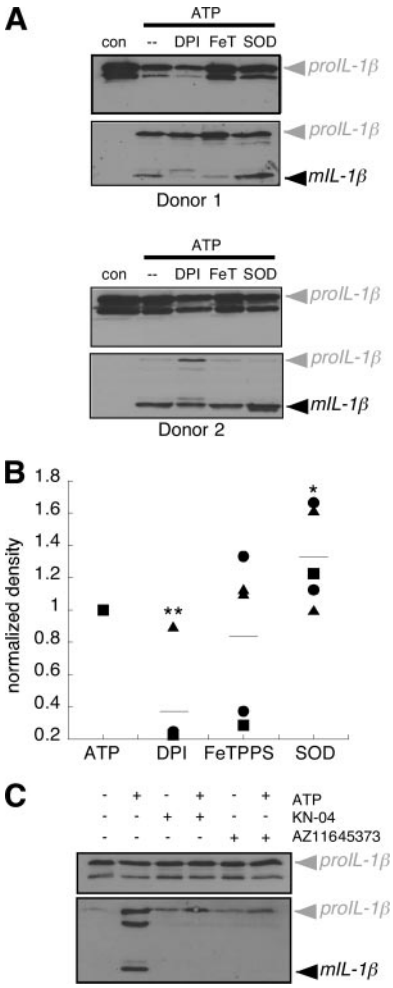

FIGURE 9. ATP stimulates oxidant-dependent IL-1β processing in human blood-derived monocytes. *A*, LPS-primed human blood-derived monocytes were incubated with inhibitors (as described in the legend to Fig. 8*A*) and then stimulated with 5 mM ATP for 45 min. Results from two different donors are illustrated as indicated. Cell lysates (*upper panel*) and concentrated secreted protein (*lower panel*) were immunoblotted for IL-1β. con, Control; FeT, FeTPPS; mIL-1β, mature IL-1β. *B*, Density measurements of the secreted active 17-kDa IL-1β band were normalized to ATP controls. IL-1β processing and secretion profiles from five different donors are represented. Data were analyzed using one-way ANOVA with Dunnett's post-test. All values are mean ± SEM; $n = 5$ separate experiments. *, $p < 0.05$; **, $p < 0.01$. *C*, LPS-primed human blood-derived monocytes were incubated with 1 μM KN-04 or 10 μM AZ11645373 for 5 min and 5mM ATP-induced (45 min) IL-1β processing and secretion were assessed by immunoblotting. Blot is representative of three separate experiments.

from inconsistent loading into monocytes derived from different donors. In primary human monocytes, $P2X_7$Rs and other purinergic receptors are coupled to robust changes in cellular oxidation that play a key role in pro-IL-1β processing in the majority of donors tested in this study. Finally, ATP-mediated IL-1β processing was attenuated by the co-addition of either 1 μM KN-04 (89% inhibition, $n = 3$) or 10 μM AZ11645373 (85% inhibition, $n = 3$), implying that the $P2X_7$R is required for maximal IL-1β processing although cellular oxidation is only partially attenuated in the presence of $P2X_7$R antagonists (Fig. 9*C*).

Discussion

Understanding the mechanisms underlying the production of bioactive IL-1β from human monocytes will be of significant importance to the development of anti-inflammatory therapies. The functional link between ATP-gated $P2X_7$Rs and the caspase-1 inflammasome is well established, yet the signaling pathways remain to be resolved. In this study we demonstrate that an oxidation-dependent post-translational modification is essential for rapid IL-1β processing in human monocytes. In agreement with previous reports, the cleavage of human IL-1β is not coupled to secretion whereby pro-IL-1β is still released in the presence of antioxidants or the inhibition of NADPH oxidase. This is the first direct demonstration that cellular oxidation is a requirement for $P2X_7$R-induced IL-1β processing in human monocytes.

Reactive oxygen species are known to play a key role in proinflammatory responses ranging from sepsis to neurodegeneration. Earlier studies have demonstrated that $P2X_7$Rs can couple to rapid changes in cellular oxidation in microglia, macrophages, and granulocytes (32, 39, 40). In the first part of this study we demonstrated that purinergic receptor stimulation leads to extracellular superoxide anion formation in endotoxin-primed human monocytes. The addition of selective human $P2X_7$R antagonists only partially reduces ATP-mediated oxidation in LPS-primed THP-1 cells and human monocytes. In THP-1 cells, ATP stimulation augments NADPH oxidase activity involving the association of $p47^{phox}$ with $p67^{phox}$ and the membrane translocation of $p67^{phox}$ in endotoxin-primed THP-1 cells blocked by a $P2X_7$R antagonist. We hypothesize that $P2X_7$Rs and other purinergic receptors may also translocate other components of NADPH oxidase (e.g., $p40^{phox}$) to modulate the NADPH oxidase activity in endotoxin-primed monocytes. We ascribe the changes in cellular oxidation to the formation of membrane-permeable peroxynitrite, a product of a fast reaction between the free radical NO and superoxide anions. Unexpectedly, incubation with NOS inhibitors did not alter the formation of peroxynitrite, suggesting an alternative source of NO. We have demonstrated that ATP-stimulated production of NO results from its displacement from intracellular *S*-nitrosothiol groups rather than from de novo synthesis. *S*-Nitrosylation and denitrosylation of cellular proteins is becoming an established signaling pathway akin to phosphorylation. It is proposed that specific enzymes regulate protein denitrosylation; these include thioredoxin reductase, protein disulfide isomerase, and calpain (36, 41, 42). The mechanism leading to the decomposition of SNO groups following ATP stimulation remains to be resolved. Overall, the current study reveals that the addition of extracellular ATP leads to the rapid formation of peroxynitrite, a powerful oxidant that would propagate the inflammatory response. Purinergic receptors, including $P2X_7$Rs, regulate a number of cellular signal-transduction pathways that are also influenced by peroxynitrite, including MAPK and metalloproteinase activation (43, 44). Indeed, $P2X_7$R-generated reactive oxygen species are reported to mediate activation of the MAPK pathway in macrophages (39). Thus, ATP-mediated peroxynitrite formation may play a fundamental role in some of the reported inflammatory actions of $P2X_7$Rs.

The most significant finding of the current study was the ability of antioxidants or the inhibition of NADPH oxidase to block the processing of IL-1β triggered by $P2X_7$Rs or nigericin (45, 46) in endotoxin-primed human monocytes. It is well established that endotoxins acting at TLR4 trigger the transcription and translation of pro-IL-1β. Extracellular ATP, acting at the $P2X_7$R, is then a potent stimulus of caspase-1 activation within the NALP3 inflammasome where receptor activation leads to the aggregation of NALP3, the recruitment of caspase-1, and the adaptor protein ASC. Active caspase-1 then cleaves pro-IL-1β at Asp^{116} to liberate a bioactive 17-kDa mature IL-1β cytokine. Rapid depletion of cytosolic potassium is the generally accepted pathway coupling $P2X_7$Rs to caspase-1 activation (18). However, it has recently been

reported that pannexin-1 inhibition blocks caspase-1 activation without influencing potassium depletion (13). This study suggested that potassium depletion alone is not sufficient to activate caspase-1. Thus, while there is strong evidence for the role of cytosolic potassium in the control of caspase-1 activity, it may not be the only signaling pathway. We present data that supports an alternative model for caspase-1 activation leading to the processing of pro-IL-1β where DPI-sensitive NADPH oxidase is required for $P2X_7R$- or nigericin-mediated IL-1β processing. The current study demonstrates that cellular oxidation, via either formation of peroxynitrite or hydrogen peroxide, is an important pathway leading to processing of IL-1β.

This study has focused specifically on the signaling mechanisms responsible for caspase-1 activation and IL-1β processing in human monocytes. Much of the evidence underpinning the concept of the inflammasome leading to caspase-1 activation has been derived from murine models (7–12). Recent studies using murine macrophages demonstrate that $P2X_7Rs$ stimulate the rapid intracellular processing of IL-1β followed by secretion (47). This is in contrast to this study and previous reports demonstrating that processed IL-1β is only detected in the external medium (13, 26). Further work is required to elucidate the role of redox signaling in the activation of caspase-1 and IL-1β processing in murine macrophages. The delayed release of IL-1β from murine macrophages may reflect different sites of superoxide anion formation (plasma membrane vs internal organelles) and, therefore, different IL-1β processing, due either to a species difference or a contrast between macrophages vs monocytes.

To conclude, two events are occurring during $P2X_7R$ stimulation that may act in concert to regulate caspase-1 activity and final IL-1β processing: oxidative stress and denitrosylation. First, oxidative stress is implicated in a plethora of signaling events from reversible inactivation of protein tyrosine phosphatases through to the assembly of the protein kinase subunits via intersubunit disulfide bonds (48, 49). Oxidative stress occurs when there is the excess production of RONS that leads to a range of reversible or irreversible protein modifications. Cysteinyl thiol groups are especially sensitive to oxidative modification and are involved in a broad range of redox-dependent signaling events. According to the location of the cysteine residue, redox-dependent modification can alter enzyme activity through to protein interactions. For nigericin stimulation, antioxidants can block caspase-1 processing without effecting the secretion of unprocessed caspase-1. These results indicate that redox inhibitors may act to prevent one of the following: 1) the activity of caspase-1, leading to an inhibition of autocatalytic processing; 2) the assembly of the inflammasome; or 3) an upstream signaling pathway leading to inflammasome activation. Although the detailed signaling pathways for oxidation-dependent activation of IL-1β processing remain to be elucidated, changes in the redox state of the monocyte is clearly an important upstream step leading to the rapid IL-1β processing resulting from NALP3 inflammasome assembly and caspase-1 activation. The second event, protein *S*-nitrosylation, can regulate a range of signaling pathways including interaction between proteins or modulation of enzyme activity. Caspase-1 has at least two potential levels of regulation by *S*-nitrosylation: modulation of protein-protein interaction within the inflammasome or *S*-nitrosylation of Cys^{285} at the active site of the enzyme. In the case of caspase-3, denitrosylation may lead to enzyme activation by either relieving interaction with an inhibitory protein or unblocking the cysteine at the active site (50, 51). Indeed, exogenous NO has been shown to inhibit the activity of caspase-1 and subsequent IL-1β processing in monocytes and macrophages (52, 53). Further studies are required to evaluate whether the temporal changes in *S*-nitrosylation play an important role in caspase-1 activation and subsequent IL-1β processing. This study introduces a new concept that ATP stimulation of human monocytes leads to the generation of oxidants that play a key upstream role in IL-1β processing subsequent to NALP3 inflammasome activation.

Acknowledgments

We thank Barry Crowley for preparation of human monocytes and Jo Carter and Catherine Hobbs for collection of blood.

Disclosures

The authors have no financial conflict of interest.

References

1. Dinarello, C. A. 1996. Biologic basis for interleukin-1 in disease. *Blood* 87: 2095–2147.
2. Li, P., H. Allen, S. Banerjee, S. Franklin, L. Herzog, C. Johnston, J. McDowell, M. Paskind, L. Rodman, J. Salfeld, et al. 1995. Mice deficient in IL-1 β-converting enzyme are defective in production of mature IL-1 β and resistant to endotoxic shock. *Cell* 80: 401–411.
3. Siegmund, B., H. A. Lehr, G. Fantuzzi, and C. A. Dinarello. 2001. IL-1 β-converting enzyme (caspase-1) in intestinal inflammation. *Proc. Natl. Acad. Sci. USA* 98: 13249–13254.
4. Wilson, K. P., J. F. Black, J. A. Thomson, E. E. Kim, J. P. Griffith, M. A. Navia, M. A. Murcko, S. P. Chambers, R. A. Aldape, S. A. Raybuck, and D. J. Livingston. 1994. Structure and mechanism of interleukin-1b converting enzyme. *Nature* 370: 270–275.
5. Walker, N. P. C., R. V. Talanian, K. D. Brady, L. C. Dang, N. J. Bump, C. R. Ferenza, S. Franklin, T. Ghayur, M. C. Hackett, L. D. Hammill, et al. 1994. Crystal structure of the cysteine protease interleukin-1 β-converting enzyme: a $(p20/p10)_2$ homodimer. *Cell* 78: 343–352.
6. Martinon, F., K., Burns, and J. F. Tschopp. 2002. The inflammasome: a molecular platform triggering activation of inflammatory caspases and processing of proIL-β. *Mol. Cell* 10: 417–426.
7. Mariathasan, S., D. S. Weiss, K. Newton, J. McBride, K. O'Rourke, M. Roose-Girma, W. P. Lee, Y. Weinrauch, D. M. Monack, and V. M. Dixit. 2006. Cryopyrin activates the inflammasome in response to toxins and ATP. *Nature* 440: 228–232.
8. Mariathasan, S., K. Newton, D. M. Monack, D. Vucic, D. M. French, W. P. Lee, M. Roose-Girma, S. Erickson, and V. M. Dixit. 2004. Differential activation of the inflammasome by caspase-1 adaptors ASC and Ipaf. *Nature* 430: 213–218.
9. Miao, E. A., C. M. Alpuche-Aranda, M. Dors, A. E. Clark, M. W. Bader, S. I. Miller, and A. Aderem. 2006. Cytoplasmic flagellin activates caspase-1 and secretion of interleukin 1β via Ipaf. *Nat. Immunol.* 7: 569–575.
10. Martinon, F., V. Pétrilli, A. Mayor, A. Tardivel, and J. Tschopp. 2006. Gout-associated uric acid crystals activate the NALP3 inflammasome. *Nature* 440: 237–241.
11. Kanneganti, T. D., N. Ozoren, M. Body-Malapel, A. Amer, J. H. Park, L. Franchi, J. Whitfield, W. Barchet, M. Colonna, P. Vandenabeele, et al. 2006. Bacterial RNA and small antiviral compounds activate caspase-1 through cryopyrin/Nalp3. *Nature* 440: 233–236.
12. Kanneganti, T. D., M. Body-Malapel, A. Amer, J. H. Park, J. Whitfield, L. Franchi, Z. F. Taraporewala, D. Miller, J. T. Patton, N. Inohara, and G. Nunez. 2006. Critical role for Cryopyrin/Nalp3 in activation of caspase-1 in response to viral infection and double-stranded RNA. *J. Biol. Chem.* 281: 36560–36568.
13. Pelegrin, P., and A. Surprenant. 2006. Pannexin-1 mediates large pore formation and interleukin-1β release by the ATP-gated $P2X_7$ receptor. *EMBO J.* 25: 5071–5082.
14. Kanneganti, T. D., M. Lamkanfi, Y. G. Kim, G. Chen, J. H. Park, L. Franchi, P. Vandenabeele, and G. Núñez. 2007. Pannexin-1-mediated recognition of bacterial molecules activates the cryopyrin inflammasome independent of Toll-like receptor signalling. *Immunity* 26: 433–443.
15. Labasi, J. M., N. Petrushova, C. Donovan, S. McCurdy, P. Lira, M. M. Payette, W. Brissette, J. R. Wicks, L. Audoly, and C. A. Gabel. 2002. Absence of the $P2X_7$ receptor alters leukocyte function and attenuates an inflammatory response. *J. Immunol.* 168: 6436–6445.
16. Chessell, I. P., J. P. Hatcher, C. Bountra, A. D. Michel, J. P. Hughes, P. Green, J. Egerton, M. Murfin, J. Richardson, W. L. Peck, et al. 2005. Disruption of the $P2X_7$ purinoceptor gene abolishes chronic inflammatory and neuropathic pain. *Pain* 114: 386–396.
17. Ke, H. Z., H. Qi, A. F. Weidema, Q. Zhang, N. Panupinthu, D. T. Crawford, W. A. Grasser, V. M. Paralkar, M. Li, L. P. Audoly, et al. 2003. Deletion of the $P2X_7$ nucleotide receptor reveals its regulatory roles in bone formation and resorption. *Mol. Endocrinol.* 17: 1356–1367.
18. Kahlenberg, J. M., and G. R. Dubyak. 2004. Mechanisms of caspase-1 activation by $P2X_7$ receptor-mediated K^+ release. *Am. J. Physiol.* 286: C1100–C1108.
19. Pétrilli, V., S. Papin, C. Dostert, A. Mayor, F. Martinon, and J. Tschopp. 2007. Activation of the NALP3 inflammasome is triggered by low intracellular potassium concentration. *Cell Death Differ.* 14: 1583–1589.
20. Sekiyama, A., H. Ueda, S. I. Kashiwamura, R. Sekiyama, M. Takeda, K. Rokutan, and H. Okamura. 2005. A stress-induced, superoxide-mediated caspase-1 activation pathway causes plasma IL-18 upregulation. *Immunity* 22: 669–677.

21. Wang, X., P. Svedin, C. Nie, R. Lapatto, C. Zhu, M. Gustavsson, M. Sandberg, J. O. Karlsson, R. Romero, H. Hagberg, and C. Mallard. 2007. *N*-Acetylcysteine reduces lipopolysaccharide-sensitized hypoxic ischemic brain injury. *Ann. Neurol.* 61: 263–271.
22. Schotte, P., G. Denecker, A. Van Den Broeke, P. Vandenabeele, G. R. Cornelis, and R. Beyaert. 2004. Targeting Rac1 by the *Yersinia* effector protein YopE inhibits caspase-1-mediated maturation and release of interleukin-1β. *J. Biol. Chem.* 279: 25134–25142.
23. Alcaraz, L., A. Baxter, J. Bent, K. Bowers, M. Braddock, D. Cladingboel, D. Donald, M. Fagura, C. Laurent, M. Lawson, et al. 2003. Novel $P2X_7$ receptor antagonists. *Bioorg. Med. Chem. Lett.* 13: 4043–4046.
24. Srivastava, S., K. Bhandari, G. Shankar, H. K. Singh, and A. K. Saxena. 2004. Synthesis, anorexigenic activity and QSAR of substituted aryloxypropanolamines. *Med. Chem. Res.* 13: 631–642.
25. Stokes, L., L. H. Jiang, L. Alcaraz, J. Bent, K. Bowers, M. Fagura, M. Furber, M. Mortimore, M. Lawson, J. Theaker, et al. 2006. Characterization of a selective and potent antagonist of human $P2X_7$ receptors, AZ11645373. *Br. J. Pharmacol.* 149: 880–887.
26. MacKenzie, A., H. L. Wilson, E. Kiss-Toth, S. K. Dower, R. A. North, and A. Surprenant. 2001. Rapid secretion of interleukin-1β by microvesicle shedding. *Immunity* 15: 825–835.
27. Andrei, C., P. Margiocco, A. Poggi, L. V. Lotti, M. R. Torrisi, and A. Rubartelli. 2004. Phospholipases C and A_2 control lysosome-mediated IL-1 β secretion: Implications for inflammatory processes. *Proc. Natl. Acad. Sci. USA* 101: 9745–9750.
28. Hempel, S. L., G. R. Buettner, Y. Q. O'Malley, D. A. Wessels, and D. M. Flaherty. 1999. Dihydrofluorescein diacetate is superior for detecting intracellular oxidants: comparison with 2′,7′-dichlorodihydrofluorescein diacetate, 5(and 6)-carboxy-2′,7′-dichlorodihydrofluorescein diacetate, and dihydrorhodamine 123. *Free Radic. Biol. Med.* 27: 146–159.
29. Possel, H., H. Noack, W. Augustin, G. Keilhoff, and G. Wolf. 1997. 2,7-Dihydrodichlorofluorescein diacetate as a fluorescent marker for peroxynitrite formation. *FEBS Lett.* 416: 175–178.
30. Aruoma, O. I., B. Halliwell, B. M. Hoey, and J. Butler. 1989. The antioxidant action of *N*-acetylcysteine: its reaction with hydrogen peroxide, hydroxyl radical, superoxide, and hypochlorous acid. *Free Radic. Biol. Med.* 6: 593–597.
31. Quijano, C., B. Alvarez, R. M. Gatti, O. Augusto, and R. Radi. 1997. Pathways of peroxynitrite oxidation of thiol groups. *Biochem. J.* 322: 167–173.
32. Parvathenani, L. K., S. Tertyshnikova, C. R. Greco, S. B. Roberts, B. Robertson, and R. Posmantur. 2003. $P2X_7$ mediates superoxide production in primary microglia and is up-regulated in a transgenic mouse model of Alzheimer's disease. *J. Biol. Chem.* 278: 13309–13317.
33. Majander, A., M. Finel, and M. Wikström. 1994. Diphenyleneiodonium inhibits reduction of iron-sulfur clusters in the mitochondrial NADH-ubiquinone oxidoreductase (complex I). *J. Biol. Chem.* 269: 21037–21042.
34. Sanders, S. A., R. Eisenthal, and R. Harrison. 1997. NADH oxidase activity of human xanthine oxidoreductase: generation of superoxide anion. *Eur. J. Biochem.* 245: 541–548.
35. Sheppard, F. R., M. R. Kelher, E. E. Moore, N. J. McLaughlin, A. Banerjee, and C. C. Silliman. 2005. Structural organization of the neutrophil NADPH oxidase: phosphorylation and translocation during priming and activation. *J. Leukocyte Biol.* 78: 1025–1042.
36. Chvanov, M., O. V. Gerasimenko, O. H. Petersen, and A. V. Tepikin. 2006. Calcium-dependent release of NO from intracellular *S*-nitrosothiols. *EMBO J.* 25: 3024–3032.
37. Hao, G., B. Derakhshan, L. Shi, F. Campagne, and S. S. Gross. 2006. SNOSID, a proteomic method for identification of cysteine *S*-nitrosylation sites in complex protein mixtures. *Proc. Natl. Acad. Sci. USA* 103: 1012–1017.
38. Alvarez, B., and R. Radi. 2003. Peroxynitrite reactivity with amino acids and proteins. *Amino Acids* 25: 295–311.
39. Pfeiffer, Z. A., A. N. Guerra, L. M. Hill, M. L. Gavala, U. Prabhu, M. Aga, D. J. Hall, and P. J. Bertics. 2007. Nucleotide receptor signaling in murine macrophages is linked to reactive oxygen species generation. *Free Radic. Biol. Med.* 42: 1506–1516.
40. Suh, B. C., J. S. Kim, U. Namgung, H. Ha, and K. T. Kim. 2001. $P2X_7$ nucleotide receptor mediation of membrane pore formation and superoxide generation in human promyelocytes and neutrophils. *J. Immunol.* 166: 6754–6763.
41. Sliskovic, I., A. Raturi, and B. Mutus. 2005. Characterization of the *S*-denitrosation activity of protein disulfide isomerase. *J. Biol. Chem.* 280: 8733–8741.
42. Nikitovic, D., and A. Holmgren. 1996. *S*-nitrosoglutathione is cleaved by the thioredoxin system with liberation of glutathione and redox regulating nitric oxide. *J. Biol. Chem.* 271: 19180–19185.
43. Bapat, S., A. Verkleij, and J. A. Post. 2001. Peroxynitrite activates mitogen-activated protein kinase (MAPK) via a MEK-independent pathway: a role for protein kinase C. *FEBS Lett.* 499: 21–26.
44. Rajagopalan, S., X. P. Meng, S. Ramasamy, D. G. Harrison, and Z. S. Galis. 1996. Reactive oxygen species produced by macrophage-derived foam cells regulate the activity of vascular matrix metalloproteinases in vitro: implications for atherosclerotic plaque stability. *J. Clin. Invest.* 98: 2572–2579.
45. Cheneval, D., P. Ramage, T. Kastelic, T. Szelestenyi, H. Niggli, R. Hemmig, M. Bachmann, and A. MacKenzie. 1998. Increased mature interleukin-1β (IL-1β) secretion from THP-1 cells induced by nigericin is a result of activation of p45 IL-1β-converting enzyme processing. *J. Biol. Chem.* 273: 17846–17851.
46. Perregaux, D., J. Barberia, A. J. Lanzetti, K. F. Geoghegan, T. J. Carty, and C. A. Gabel. 1992. IL-1β maturation: evidence that mature cytokine formation can be induced specifically by nigericin. *J. Immunol.* 149: 1294–1303.
47. Brough, D., and N. J. Rothwell. 2007. Caspase-1-dependent processing of pro-interleukin-1β is cytosolic and precedes cell death. *J. Cell Sci.* 120: 772–781.
48. Brennan, J. P., S. C. Bardswell, J. R. Burgoyne, W. Fuller, E. Schröder, R. Wait, S. Begum, J. C. Kentish, and P. Eaton. 2006. Oxidant-induced activation of type I protein kinase A is mediated by RI subunit interprotein disulfide bond formation. *J. Biol. Chem.* 281: 21827–21836.
49. Burgoyne, J. R., M. Madhani, F. Cuello, R. L. Charles, J. P. Brennan, E. Schröder, D. D. Browning, and P. Eaton. 2007. Cysteine redox sensor in PKGIα enables oxidant-induced activation. *Science* 317: 1393–1397.
50. Matsumoto, A., K. E. Comatas, L. Liu, and J. S. Stamler. 2003. Screening for nitric oxide-dependent protein-protein interactions. *Science* 301: 657–661.
51. Mitchell, D. A., and M. A. Marletta. 2005. Thioredoxin catalyzes the *S*-nitrosation of the caspase-3 active site cysteine. *Nat. Chem. Biol.* 1: 154–158.
52. Fiorucci, S., L. Santucci, G. Cirino, A. Mencarelli, L. Familiari, P. D. Soldato, and A. Morelli. 2000. IL-1 β converting enzyme is a target for nitric oxide-releasing aspirin: new insights in the anti-inflammatory mechanism of nitric oxide-releasing nonsteroidal anti-inflammatory drugs. *J. Immunol.* 165: 5245–5254.
53. Kim, Y. M., R. V. Talanian, J. Li, and T. R. Billiar. 1998. Nitric oxide prevents IL-1β and IFN-γ-inducing factor (IL-18) release from macrophages by inhibiting caspase-1 (IL-1β-converting enzyme). *J. Immunol.* 161: 4122–4128.